Cellulose (2023) 30:4293–4314
https://doi.org/10.1007/s10570-023-05163-2

ORIGINAL RESEARCH

Improved degradability and mechanical properties of bacterial cellulose grafted with PEG derivatives

Edina Rusen · Gabriela Isopencu · Gabriela Toader · Aurel Diacon · Adrian Dinescu · Alexandra Mocanu

Received: 24 October 2022 / Accepted: 20 March 2023 / Published online: 4 April 2023

Abstract New functional materials based on bacterial cellulose (BC) grafted with poly(ethylene glycol) PEG derivatives for food packaging applications and a facile method for assessing the degradation rates of the final materials are presented. Two types of materials were obtained by grafting the BC films (BCF), respectively lyophilized BC pellicles (BCL) with three PEG derivatives of different molecular weights through radical polymerization. The BC based polymer materials were characterized by SEM, FT-IR, contact angle measurements, and TGA. Tensile tests and DMA analysis were used to compare the two types of materials in terms of shear-modulus, tensile strength and performance giving suitable information for food packaging applications. A new degradation evaluation method, that we propose herein, offers quantitative information about the degradation process in contrast with the SEM analysis, primarily used in literature, which is not decisive in all cases because it characterizes only small parts of the sample. The degradation rates evidenced that the PEG derivatives of higher molecular weight grafted on the surface of BCF led to an acceleration of the degradation process compared with the pristine samples. A good correlation was obtained between the samples analyzed by SEM after the degradation process and their degradation rates were mathematically determined.

Keywords Bacterial cellulose · PEGDA · PEGMA · Mechanical test · Degradation test · Food packaging

Edina Rusen and Gabriela Isopencu contributed equally to this work.

Supplementary Information The online version contains supplementary material available at https://doi.org/10.1007/s10570-023-05163-2.

E. Rusen · G. Isopencu · A. Diacon · A. Mocanu (✉)
Faculty of Chemical Engineering and Biotechnologies, University Politehnica of Bucharest, 1- 7 Gh. Polizu Street, 011061 Bucharest, Romania
e-mail: alexandra.mocanu@upb.ro

G. Toader · A. Diacon
Military Technical Academy "Ferdinand I", 39-49 George Cosbuc Av., 050141 Bucharest, Romania

A. Dinescu
National Institute for Research and Development in Microtechnologies (IMT-Bucharest), 126 A, Erou Iancu Nicolae Street, 023573 Bucharest, Romania

Introduction

Nowadays, about 99% of plastic packages are manufactured from petroleum-based polymers due to their unique properties such as low weight, low costs, facile processing, high resistance to environmental conditions and high versatility in terms of applications (Byun and Kim 2014; Mülhaupt 2013). The greatest disadvantages of these packages are related to their low biodegradability and in many

cases to the lack of recycling technologies in the case of thermosets plastics. Thus, in the food and beverage industry most of the packages are used only once and only 10% end up being recycled, while another 10% are incinerated and 80% are disposed to landfills (Mülhaupt 2013; Zhao et al. 2020).

The pressure imposed by the new and more severe environmental regulations and the increase in the consumer awareness for reducing CO_2 emissions could determine a scientific and technological change in the future of "greener" processes or products. Thus, the necessity to live in a cleaner, sustainable environment could lead to an industry manufacturing progress based on the idea "if it's not recyclable then it should not be produced". Starting from this idea, the global market for bioplastics started to be known from the activities of European and Asian manufacturers 5 years ago when it reached 1% of the total plastic market (Hong et al. 2021). According to Zhao et al. (2020) an increase of 40% market share is expected by 2030 due to the dramatic climate change determined by pollution and fossil-fuel dependency.

Considering these issues, the use of renewable and biodegradable materials will continuously grow. For this reason, many researchers have drawn their attention to biodegradable materials to build up new bioplastics (Siracusa et al. 2008).

Commercial bioplastics produced by different companies are based on different natural biopolymers like poly(lactic acid) (PLA), poly(hydroxyalkanoates) (PHA), polybutylene succinate (PBS), starch, cellulose and blends thereof (Bhardwaj et al. 2014; Khan et al. 2017; Siracusa et al. 2008; Zhao et al. 2020) due to certain properties like increased mechanical strength, low density, low thermal expansion coefficient, biodegradability and biocompatibility (Mokhena and John 2020; Zhao et al. 2020) necessary for food packaging or medical applications.

Cellulose is one of the most common choices to produce bioplastics due to some advantages that come from its polysaccharide structure composed of β-D-glucopyranose units linked by β-1,4-glycosidic bonds and its high density of hydroxyl groups present on the polymeric chain (Ghaderi et al. 2014; Moon et al. 2011). The exploitation of cellulose from wood, cotton and other plants is sometimes difficult, energy consuming and costly since its structure is associated with hemicellulose and lignin that need to be separated (Chen et al. 2019; Dong et al. 2014; Sun and Tomkinson 2005).

Since there are enormous efforts to protect forests from severe exploitation cellulose production was directed to microbial synthesis of bacterial cellulose (BC).

Bacterial cellulose (BC) produced extracellularly by different *Gram-negative* bacterial cultures of *Gluconacetobacter*, *Acetobacter*, *Agrobacterium*, *Achromobacter*, *Aerobacter*, *Sarcina*, *Azobacter*, *Rhizobium*, *Pseudomonas*, *Salmonella* and *Alcaligenes*(Jang et al. 2019; Marič et al. 2020; Zhang et al. 2017a) has proven to be one of the purest forms of cellulose being constituted from (1→4)-D-glucopyranose units linked together by β-glycosidic bonds just like cellulose but without lignin, hemicellulose, pectin or wax normally present in plants.

Fundamentally, the BC is a linear natural polymer in which glucose monomer units are joined through a β-1,4 linkage totalizing approximately 15 000 molecules per each chain (Tsouko et. al. 2015; Raghavendran et. al. 2020). This represents a great advantage in terms of industrial production of BC since it does not need costly separation or purifying stages for its further use.

The industrial production of BC has been slow ever since it was discovered in 1970s. This was attributed to the high sensitivity of the acetic strains to stirring process and low temperature fermentation conditions. Some of these issues have currently been resolved by Hainan Yeguo Foods Co. Ltd. (Zhong 2020). This company is one of the biggest manufacturers of BC products in the world supplying BC for a great range of applications including food products, medical and personal care products, a replacement for paper and packaging,, textiles, and composite materials (Blanco Parte et al. 2020; Zhong 2020).

The versatility of BC in terms of applications is strongly related to its physical and chemical structure that confers unique characteristics such as high degree of crystallinity, high purity, high water retention (up to 98% wt.), high mechanical strength, and enhanced biocompatibility (Blanco Parte et al. 2020).

Other advantages coming from BC structure are related to the possibility of biological, physical and chemical modification of the natural polymer membranes by different methods such as: i) surface treatment; ii) blending; iii) molecular modification; iv) modification of pore structure and v) polymer

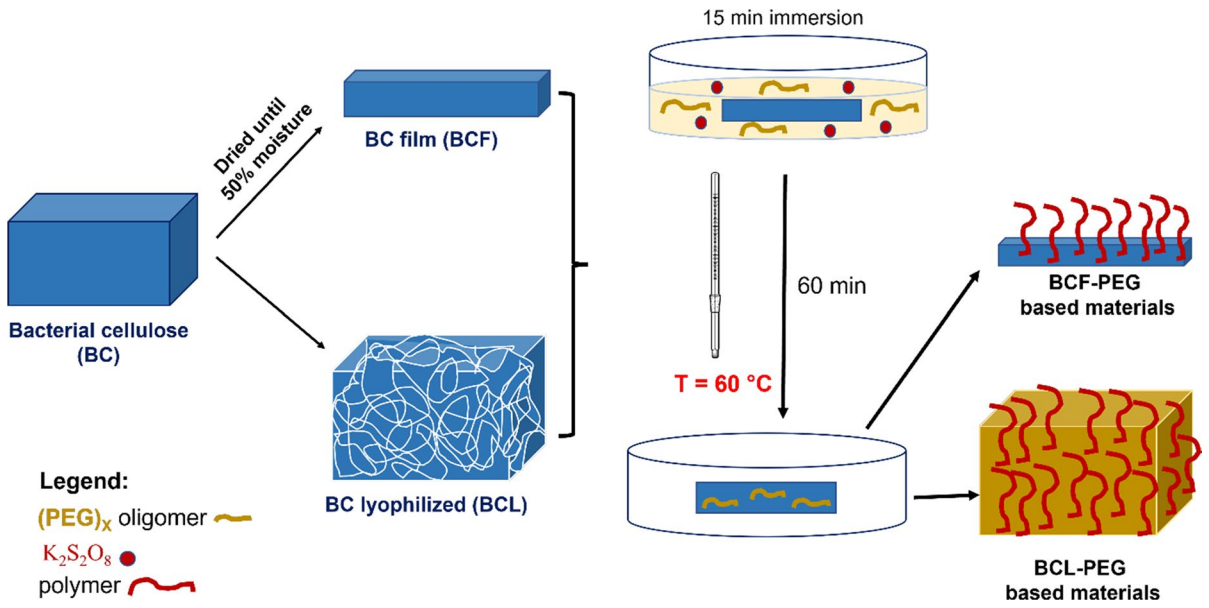

Scheme 1 The synthesis procedure of BCF, respectively BCL-PEG based materials

grafting (Choi and Shin 2020; Li et al. 2017; Vadanan et al. 2022; Zhijiang et al. 2012).

Of all these methods, polymer grafting is facile, offering significant advantages for BC modification by enabling new properties of the final materials that the individual compounds fail to exhibit (Chen et al. 2022).

Based on these remarks, our first aim was to chemically modify BC pellicles resulted from static culture by grafting poly(ethylene glycol) methyl ether methacrylate (PEGMA) or poly(ethylene glycol) diacrylate (PEGDA) with different molecular weights to obtain materials with improved mechanical properties and biodegradability for possible food packaging applications. Thus, by employing radical polymerization in the presence of BC pellicles or lyophilized BC, polymer chains of PEGDA 700, PEGMA 475 and PEGMA 1100 were grafted on the fibrils of BC (Scheme 1). The choice of these reactive oligomers is related to their inactivity towards different bacteria strains and their biocompatibility characteristics (Kongkaoroptham et al. 2021; Moore and West 2019; Morris et al. 2017; Wang et al. 2001) which represents a good premise for food packaging or biomedical applications. A special attention was given to the materials based on lyophilized BC modified with the above-mentioned oligomers. The resulted materials were analyzed by SEM, FT-IR, contact angle measurements tensile tests, TGA, and DMA.

To prove that these materials are biodegradable, a degradation test was performed in the presence of three types of molds generally encountered on fruits surface since food packaging applications were targeted.

Thus, our second aim was to give a supplementary interpretation of the degradation process by plotting the weight of the samples exposed to molds versus time, considering that SEM analysis greatly used in literature data to prove the degradation behavior of different materials is not enough, SEM micrographs evaluating only small parts of the sample. This method served for a better comparison between all samples since the degradation rates were expressed as mass loss versus time. To our knowledge, this is the first time when this method is proposed to evaluate the degradation process of biodegradable materials. Nevertheless, SEM micrographs were also used to confirm the degradation results of the samples exposed for 7 days to the three types of molds *(Trichoderma viridae, Sporotrichum pulverulentum and Fusarium oxysporum)*.

Materials and methods

Materials

BC membranes were obtained by static culture in Mass Transfer Laboratory of University Politehnica of Bucharest according to the method described in Sect. "Synthesis of bacterial cellulose". Poly (ethylene glycol) diacrylate (PEGDA) (Mn = 700 g/mol) and poly (ethylene glycol) methyl ether methacrylate (PEGMA) (Mn = 475 g/mol, respectively Mn = 1100 g/mol) assigned as PEGDA700, PEGMA475, and PEGMA1100 were purchased from Sigma-Aldrich and used as such. Potassium persulfate ($K_2S_2O_8$) (KPS) (Merck) has been recrystallized from an ethanol/water mixture and then vacuum-dried until constant mass.

Methods

Synthesis of bacterial cellulose

BC was obtained in static culture by employing a modified method of Hestrin–Schramm [MHS] culture medium as in our previous study (Dobre et al. 2008; Mocanu et al. 2019). Wastes of forest fruits with 2% wt. carbon source were used for the growth of *Gluconacetobacter strain* at 28 °C. After 10 days the BC membranes were purified using aqueous solution of NaOH 0,5 N at 90 °C for 1 h and then rinsed repeatedly with deionized water until neutral pH to make sure the acetic bacteria were inactivated and removed.

Lyophilization of BC membranes

The purified BC membranes of 10 X 10 cm^2 were first frozen to -18 °C and after 24 h introduced in BIOBASE BK-FD10S equipment at − 60 °C and 10 Pa with condensation capacity of 1 kg/12 h. The lyophilized samples were removed after 24 h, used as such and encoded BCL.

Synthesis of BCL-polymer materials

The preparation of BCL-polymer materials involved cutting the BCL membrane into samples of 10 mm X 100 mm. Aqueous solutions with a monomer concentration of 6.9 X 10^{-4} M were prepared for the modification of BCL with a layer of polymer. Thus, 0.48 g of PEGMA700, 0.33 g of PEGMA475, respectively 0.76 g of PEGMA1100 were dissolved in 12 mL deionized water in which 0.1 g of $K_2S_2O_8$ were added. The BCL samples were immersed in the aqueous solutions of acrylic monomers and initiator for 15 min. After removal of the samples from the solutions the polymerization was performed at 60 °C for 1 h. The BCL-polymer materials were washed several times with water to remove the unreacted monomers and then dried at 50 °C until constant mass. The samples were assigned as BCL for blank, BCL-PEGDA700, BCL-PEGMA475 and BCL-PEGMA1100.

Synthesis of BCF-polymer materials

After purification of BC, the membranes were dried to half of their mass and then impregnated with aqueous solutions of the three acrylic polymers. The samples were dried until half of their mass, using thermogravimetric equipment. The solutions were prepared by dissolving 0.24 g of PEGMA 700, 0.165 g of PEGMA475, respectively 0.38 g of PEGMA 1100 in 6 mL of deionized water in which 0.05 g of $K_2S_2O_8$ were added. The impregnated films were then polymerized at 60 °C for 1 h. The resulting BC-polymer films were cut in samples of 10 mm X 10 cm and assigned as BCF for blank, BCF-PEGDA700, BCF-PEGMA475 and BCF-PEGMA1100.

Degradation tests of BC-polymer based materials

The microbiological study aimed the degradation of pristine BC and reinforced BC by the three different types of polymers. Thus, three cellulase-producing strains were selected: *Trichoderma viridae*, *Fusarium oxysporum* and *Sporotrichum pulverulentum.* The strains were isolated from the soil, characterized and included in the library of the laboratory of Industrial Microbiology of the Faculty of Chemical Engineering and Biotechnologies from University "Politehnica" of Bucharest. The molds were grown on solidified PDA medium (purchased from Sigma-Aldrich). The inoculation technique implied a flooding procedure with a spore suspension with a concentration of 1.5×10^8 spores/mL. The BC-polymer based samples were cut into rectangular pieces with dimensions of approx. 10 X 7 (± 1 mm), weighed and sterilized by UV (wavelength of 254 nm) for 15 min. After sterilization,

the samples were placed on the surface of the solid medium inoculated with the spore suspension. Incubation was performed at 30 °C, and complete invasion of the petri dish by the mold mycelium took place after 3 days.

Invasion of the mold hyphae occurred also on the BC polymer samples, to a greater extent by *S. pulverulentum*, followed by *T. viridae*, while *F. oxysporum* did not show a direct mycelium increase on the sample, instead changing its color in dark cherry and increasing its moisture content.

After 7 and 34 days respectively, of direct contact of the samples with the mould strains, the BC samples were extracted from the nutrient medium and maintained in the same incubation conditions and constant humidity of the storage chamber in order to favor an increase or maintenance of the mold on the surface of the samples. In this case, the molds will receive glucose as the only carbon source from BC and nitrogen from atmospheric environment.

To investigate the degradation behavior of the blank and BC-polymer based materials the samples were weight at 7, 14, 34, 45 and 80 days after exposure to molds. The mass loss was plotted against time to obtain the degradation rate of the samples. The degradation rate was determined mathematically as the slope of the degradation curves.

Characterization

SEM analysis

The morphologies of the materials were investigated through field emission gun scanning electron microscope (FEGSEM) Nova NanoSEM 630 (FEI) (Hillsboro, OR, USA). To achieve conductive surfaces, the BC-polymer samples were coated with a thin layer of gold (few nm) by DC sputtering. The SEM images were recorded at 10 kV.

Fourier transforms infrared spectroscopy (FT-IR) analysis

FT-IR analysis was performed on a Spectrum Two FT-IR Spectrometer (Perkin Elmer), equipped with a universal ATR–MIRacle™ Single Reflection ATR–PIKE Technologies, at 4 cm^{-1} resolution, from 550 to 4000 cm^{-1} and a buildup of 32 scans.

Contact angle measurements

To determine the hydrophilic nature of the BCF-polymer materials contact angles have been measured with a EW-59780-20 Contact Angle Meter 110 VAC, 50/60 Hz. A drop of water was deposited on the BCF blank and BCF-polymer films; the contact angle was calculated after recording 1 frame at every 5 s for 2 min.

Mechanical tests

The mechanical properties of the thin BCF-polymer based materials were investigated on a Discovery 850 DMA TA Instruments, by using two different setups: s*hear-sandwich clamp* for evaluating the frequency-dependent shear modulus and *tensile test clamp* designed for uniaxial deformation investigations. For the **shear-sandwich** setup, two equal-size square shaped pieces of the same material (12 mm × 12 mm × 0.1 mm–0.4 mm) were sheared between two fixed plates and a moving plate, for the measurement of shear modulus. To obtain a good adherence between the samples and the clamps, a compressive pre-strain of 1% was applied. **Tensile tests** were performed on rectangular specimens (40 mm × 5 mm × 0.1 mm–0.4 mm), at 5 mm/min, on the same Discovery 850 DMA TA Instruments, by using this time the tensile test clamp for thin films. Triplicate tests were performed, and the mean values were reported. Due to the geometry of the instrument, the maximum extension of the samples is restricted, therefore some samples may not break. Even so, the high accuracy of this performant instrument allowed a precise comparison between the evaluated samples.

For evaluating the value of the maximal stress (at break), the same samples were also subjected to another set of tensile tests, on a different instrument. Thus, the second set of tensile tests were performed on a Titan 2 universal strength-testing machine equipped with a 600 N force cell. From each type of sample, rectangular shaped specimens (10 mm × 100 mm), having thicknesses which varied between 0.1 and 0.4 mm, were subjected to tensile tests at a speed of 5 mm/min. To be able to compare the results, the mean values for each sample were plotted in a stress/strain multigraph. Five specimens from each sample were subjected to this second set of tensile tests.

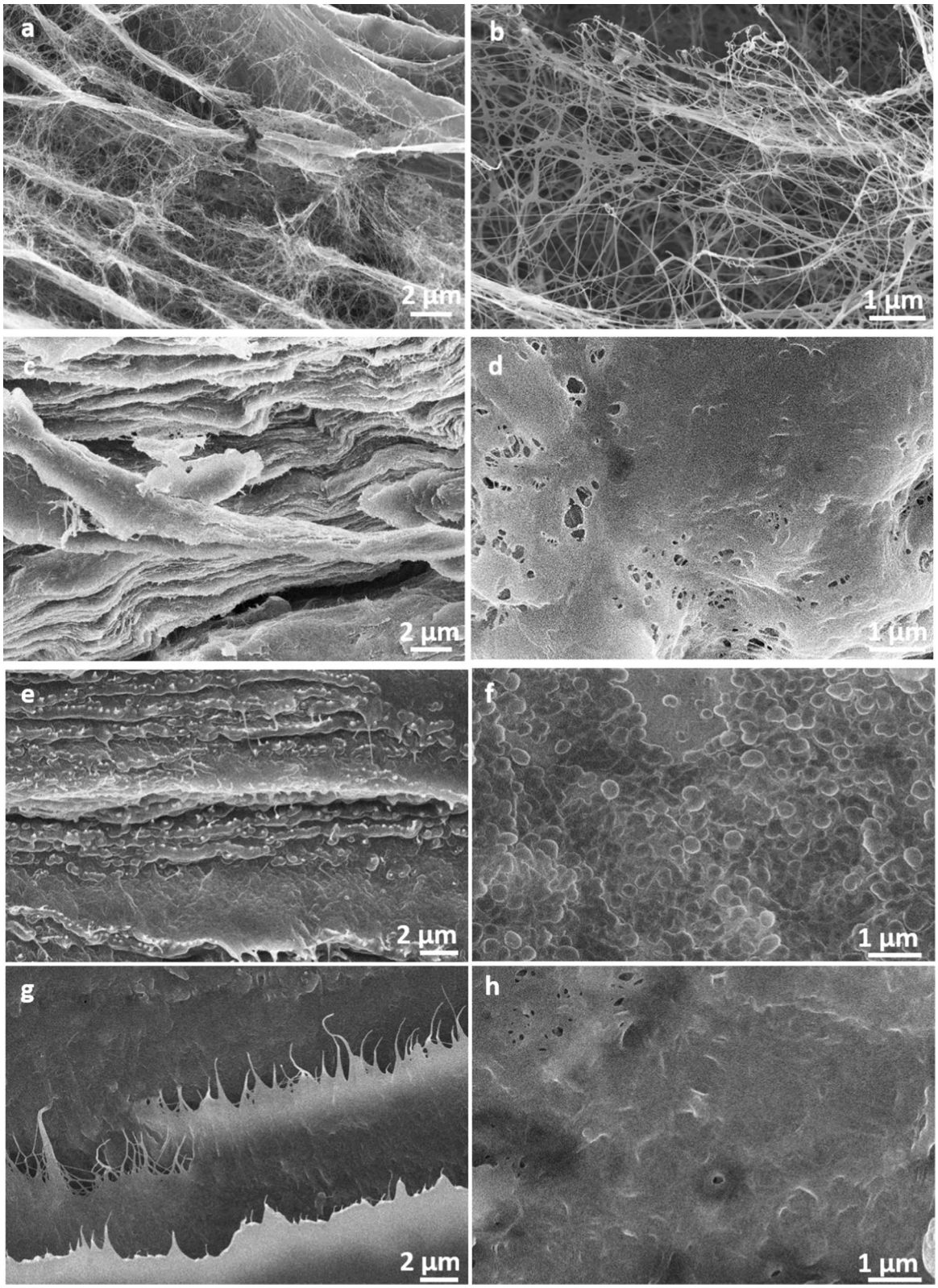
a
2 µm
b
1 µm
c
2 µm
d
1 µm
e
2 µm
f
1 µm
g
2 µm
h
1 µm

◂**Fig. 1** SEM micrographs in cross-section **a**, **c**, **e**, **g**, respectively top of the composite materials **b**, **d**, **f**, **h** for BCL**,** BCL-PEGDA700, BCL-PEGMA475, and BCL-PEGMA1100

DMA single cantilever measurements

Were performed on a DMA Discovery 850 From TA Instruments to determine the thermo-mechanical properties of the samples in order to evaluate their potential as future packaging materials. Thus, samples of 36 mm x 12 mm x approx. 0.5 mm were subjected to analysis, being heated from − 30 °C to + 115 °C, with 5 °C/min heating rate.

Thermogravimetric analysis (TGA)

The thermogravimetric analyses (TGA) of the pristine and modified BC were performed using a Netzsch TG 209 F3 Tarsus equipment considering the next parameters: nitrogen atmosphere flow rate 20 mL min^{-1}; samples mass: ~ 3 mg; temperature range: room temperature − 900 °C; heating rate: 10 °C min^{-1} in an alumina (Al_2O_3) crucible.

Degradation tests

To analyze the degradation performance of the BC and BC-polymer based materials, we proposed a correlation between graphical, and mathematical method in which the mass loss of the samples (exposed to the three types of molds) was plotted versus time and the degradation rate (the slope of the curve) was determined using the tendency lines; for the interpretation of the results the values of the slopes in module were considered.

In order to correlate the results obtained by the proposed method, the aspect of the samples exposed to the three types of molds for 7 days were analyzed by SEM micrographs.

Results and discussions

SEM analysis of BC-polymer materials

The blank samples, BCL and BCF as well as the functional materials resulted after grafting the PEG derivatives were first analyzed by SEM in order to investigate the aspect of the samples before and after the modification process.

As depicted in Fig. 1a, c, e and g the samples were analyzed in cross-section to examine their morphology. The samples resulted from lyophilized BC had a more compact aspect as the molecular weight of the oligomers increased and a coat of polymer covering the fibers was noticed in all cases. Thus, for BCL a porous 3D fibrous structure was identified both on top and in cross-section of the sample (Fig. 1a, b). In the case of grafting the highest molar weight of the PEG derivatives the BCL fibers were almost completely covered by polymer (Fig. 1g, h). An interesting morphology was obtained in the case of BCL-PEGMA475 that presented polymer particles grafted onto the surface of the BCL (Fig. 1f—top image), while in cross-section almost a full coverage of the fibers was noticed (Fig. 1e).

Following the same reasoning, the BC-polymer based samples resulted from BCF were analyzed by SEM.

The morphology of BCF is more compact (Fig. 2a) than the lyophilized one with few separated fibers in cross-section (Fig. 2b—detail image). Compared with previous samples, the ones resulted from BCF have a strong compact aspect with no pores or hollows in the structure of BC-polymer based materials regardless of the polymer grafted from the BC membrane. The same behavior for samples modified with PEGMA475 was noticed. Figure 2e, f revealed a BCF covered with close-packed particles for BCF-PEGMA475 similar to the BCL-PEGMA475 (Fig. 1e, f).

FT-IR analysis

FT-IR analysis was performed for all samples regardless of their BC support (lyophilized or film) and similar results were obtained for both blank and modified samples. For both BCL and BCF the characteristic cellulose peaks were obtained as expected at 3339 cm^{-1} for O–H stretching vibrations, at 2894 cm^{-1} for C–H stretching vibrations, at 1456 cm^{-1} for C–H bending vibrations and 1050 cm^{-1} for C–O–C stretching vibrations in good agreement with literature data (Numata et al. 2021).

The characteristic vibration of hydroxyl groups of BC pristine substrate registered at 3339 cm^{-1} was

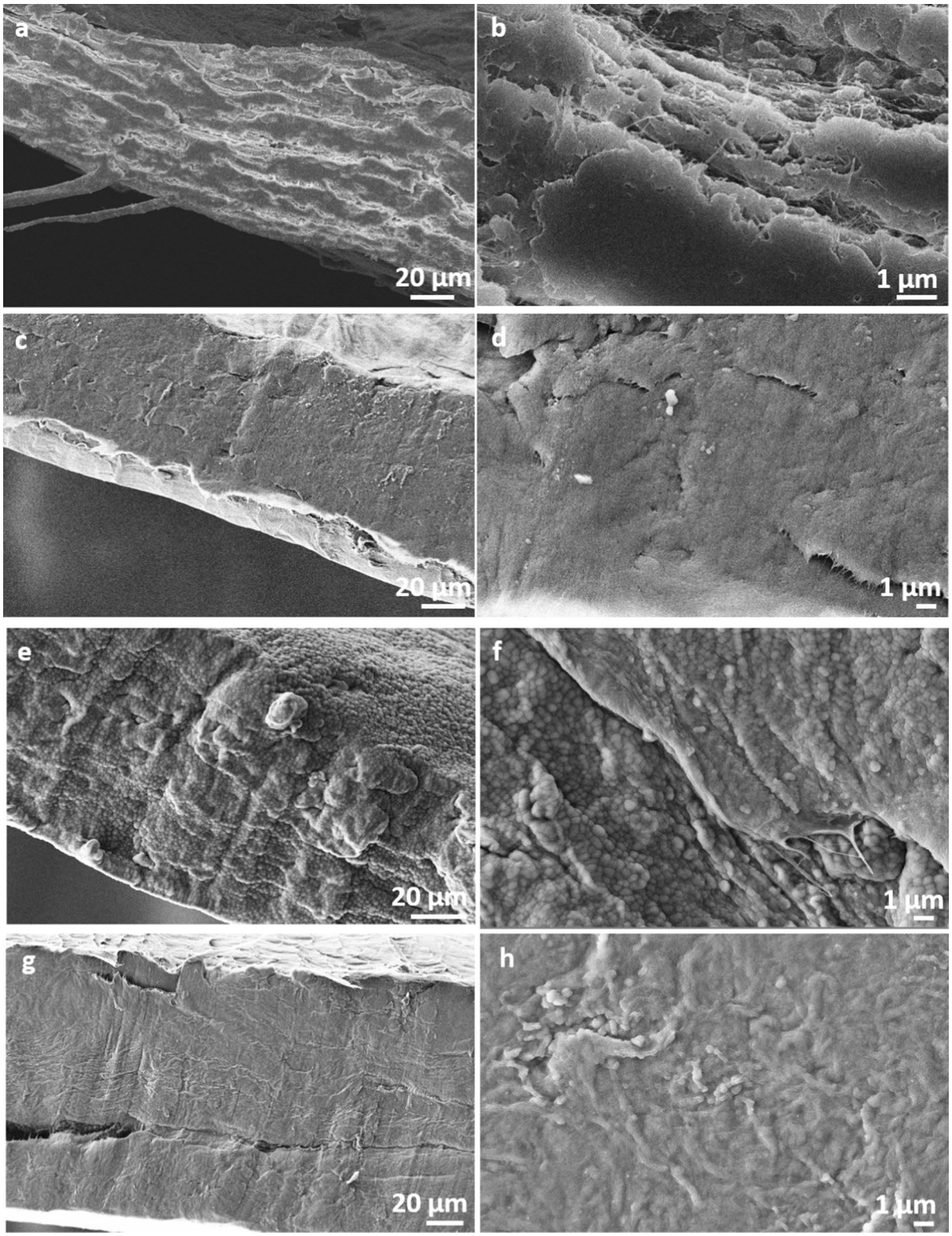

Fig. 2 SEM micrographs in cross-section at two different scales (20, respectively 1 µm) for BCF (**a, b**), BCF-PEGDA700 (**c, d**), BCF-PEGMA475 (**e, f**), and BCF-PEGMA1100 (**g, h**)

shifted in the BC-polymer based spectra at 3348 cm^{-1} for grafted PEGDA700, 3352 cm^{-1} for PEGMA475, respectively 3286 cm^{-1} for PEGMA1100 due to the interaction of –OH groups from both BC and polymer chains. Also, the presence of –OH groups in the polymers led to a broadening and intensity increase of the peak as the molecular weight of the PEGMA grafted chains was increased compared with BC blank samples. The same results were obtained for the characteristic peak at 2894 cm^{-1} of C–H stretching vibration for pure cellulose that was shifted to 2875 cm^{-1} for the polymer modified BC in all cases (Cai and Kim 2010). In the case of BC-based polymer materials, a clear peak was registered at 1628 cm^{-1} confirming the characteristic band derived from acrylate double bonds confirming the grafting onto the BC fibers (Numata et al. 2017). The BC-polymer modified samples registered at 1089 cm^{-1} a sharp peak corresponding to the –C = O acrylic bond (Numata et al. 2015). In the case of PEGMA grafted chains onto BCL or BCF the intense peak at 1101 cm^{-1} is attributed to the C–O–C aliphatic ether bond (Zhang Xiuqiang et al. 2017b). The intensity of the peak increased as the molecular weight of the PEGMA chains was increased.

Contact angle measurements

To determine the hydrophilic nature of the materials, contact angle measurements were performed for the BCF-polymer materials (images are depicted in *Supplementary info*—Figure S1). Thus, Table 1 summarizes the values obtained for the blank BCF, BCF-PEGDA700, BCF-PEGMA475, and BCF-PEGMA1100.

Compared with the blank sample, BCF-PEGDA700 has a slightly higher value of the contact angle which is also superior to the other two BCF samples modified with PEGMA of different molar weight. This could be attributed to the reactivity of PEGDA, which has two double polymerizable bonds compared with the other oligomers making it more reactive. On the other hand, BCF-PEGMA1100 has a smaller value of the contact angle compared with BCF-PEGMA475 which can be attributed on one hand to a higher grafting degree of PEGMA1100 compared with PEGMA475 and probably to the different morphology of the two samples analyzed by SEM (Fig. 2). Thus, the increase in molar weight in the case of PEGMA475 and PEGMA1100 did not drastically changed the values obtained for the contact angle measurements, the two samples having almost the same hydrophilic behavior.

For the BCL-polymer based samples, due to the higher porosity of the specimens (confirmed by the SEM analysis Fig. 1), the contact angle measurements were inconclusive, displaying a high degree of uncertainty.

Table 1 Contact angle measurements for BCF-polymer based materials

Sample code	Contact angle values
BCF	74.91 ± 2.6°
BCF-PEGDA700	76.82 ± 4.75°
BCF-PEGMA475	47.15 ± 5.82°
BCF-PEGMA1100	46.75 ± 4.3°

Mechanical tests

Shear-sandwich setup on Discovery 850 DMA TA Instruments

The viscoelastic properties of the BCF-based polymer materials were evaluated with the aid of a shear-sandwich setup (Figure S2—*Supplementary information*) consisting of parallel plates, in frequency sweep mode used to determine the storage (G′) and loss (G″) moduli as function of frequency (Rebelo et al. 2018).

As can be observed from Fig. 3, the viscoelastic properties followed comparable patterns which varied in accordance with the effects induced by the polymers employed in the synthesis of the BC films. The variation of shear moduli as a function of frequency offers information on the "damping" behavior of BC films by illustrating their ability to dissipate mechanical energy through internal motion (Dîrloman et al. 2021). In all cases, all samples registered higher values of G' storage modulus and lower values for G'' loss modulus in the whole frequency range. By comparing the results obtained in Fig. 3a, we can affirm that the grafting of PEGMA1100 chains onto BC fibers had the most significant influence on the storage and loss modulus on BC films, probably due to its longer polymeric chains compared with the other PEG derivatives which considerably modified internal motion within the BC film. BCF-PEGMA1100

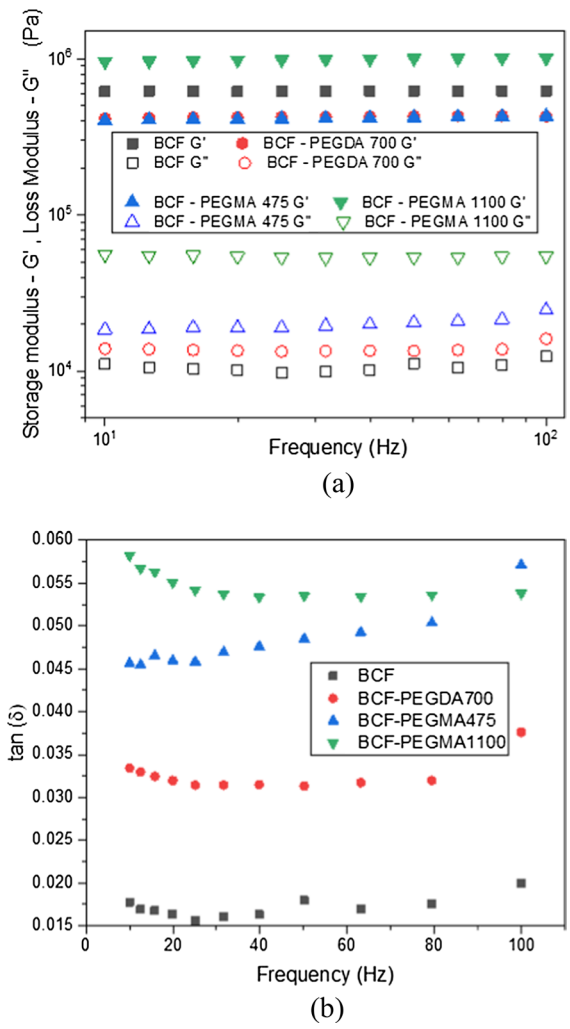

Fig. 3 The viscoelastic properties of BCF-based materials: Storage modulus (G') and loss modulus (G") **a**, and tan delta (δ) values **b** as a function of frequency

has also been the only sample that exhibited a slight decrease of tan delta (Fig. 3b) values at higher frequencies probably due to the slower and more gradual slippage displayed by the longer chains of PEGMA1100 when shear stress was applied.

The storage modulus was lower for PEGDA700 and PEGMA475 grafted chains compared even with the BCF blank sample which can be attributed to the shorter chain length or a lower grafting degree that led probably to conformational changes of the final materials and a more rigid behavior of BCF-PEGDA700 and BCF-PEGMA475 (Fig. 3a). Nevertheless, for all the evaluated samples, their ability to dissipate mechanical energy while shear stress was applied, was reflected in their "damping" abilities.

Tensile test setup on Discovery 850 DMA TA Instruments

The second type of analyses performed for evaluating the mechanical properties of BC films and lyophilized BC modified with PEG derivatives consisted in utilizing a tensile test clamp (set-up presented in Figure S3—*Supplementary information*) designed for uniaxial deformation investigations on the same Discovery 850 DMA instrument mentioned above.

The results obtained were comparatively shown in Fig. 4 and Table 2. It is worth mentioning that this method presented a small disadvantage, represented by the maximal force of this instrument which was 18N, and the maximum extension of the samples which is restricted to 25 mm due to the geometry of the instrument, as can be observed in Figure S3 in *Supplementary information*. Nevertheless, its high accuracy offered reasonable evidence of the reproducibility of the evaluated specimens from each sample and fair comparison between their mechanical performances. Thus, in the case of this instrument, the analysis ended when the maximal overload was reached, but valuable information was however obtained. As can be observed from Fig. 4, all three types of polymers used for the synthesis of BC-polymer based materials brought significant improvements in terms of mechanical resistance. BCF-PEGMA475, being the shorter polymeric chain employed for the modification of BC film, induced a higher mechanical resistance but lower stretchability in comparison with neat BC films (blank/reference sample), while its analogue with longer chains, PEGMA 1100, led to optimal mechanical performances, possessing both high resistance and also a slightly higher stretchability (Fig. 4a). In contrast, BCF-PEGDA700 specimens displayed a mechanical resistance comparable to the one of BCF-PEGMA475, probably as a result of the proprieties induced by its two reactive sites. Table 2 offers complementary information on the evaluation of the mechanical performances obtained for both types of samples subjected to analysis. The stress values were compared at the same strain value ($\varepsilon = 0.25\%$) and the results are in accordance with the assumptions made based on the chemical structure

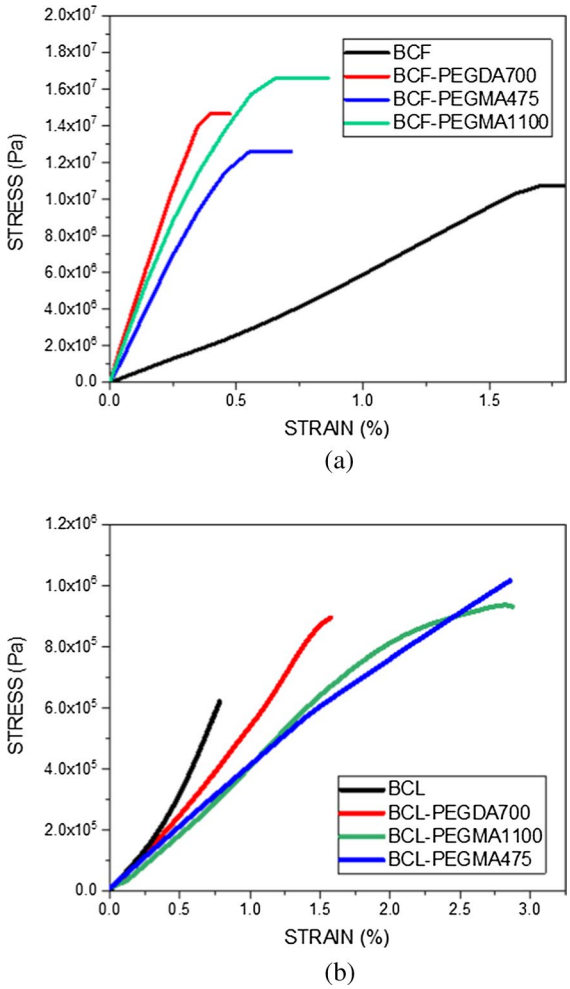

Fig. 4 Comparative stress–strain plots for BCF-based samples **a** and BCL-based specimens **b** obtained by utilizing the tensile test clamp setup on Discovery 850 DMA TA Instruments

of the oligomers employed for the synthesis of these new materials.

When compared to equivalent specimens, the stress value recorded at = 0.25% for BCL-polymer based films (Fig. 4b) was significantly diminished, and the Young Modulus was two orders of magnitude lower (Table 2). In this case, all samples modified with PEG derivatives induced higher stretchability compared with BCL blank. This could be explained by the porous morphology of the BCL substrate that allowed the protrusion of PEG chains during polymerization reaction and possible chain conformational changes. Thus, as presented in Fig. 4b, best results in terms of mechanical performance and stretchability were registered by BCL-PEGMA475 and BCL-PEGMA1100.

Tensile test setup on Titan 2 Instrument

Specimens from the same samples were also subjected to tensile tests on a second instrument, Titan 2, which allowed the extension of the specimens until break. On this instrument, two types of samples were tested: the same thin BC films that were also tested on Discovery 850 DMA Instrument and also analogous BC films which were lyophilized previously.

In Fig. 5 comparative strain–stress plots between the samples resulted from the modification of BC lyophilized or BC film were presented. Even if the blank sample displayed a higher strain value in Fig. 5a the modification of the BCF with different types of polymeric matrices led to higher stress values, which means that the addition of these polymeric into BC matrices led to enhanced mechanical performances. Thus, the fracture stress of the BCF-polymer based materials increased from 8.8. MPa for the pristine BCF up to 27 MPa for the BCF-PEGMA475. These values are considerably higher than other results from literature data in which BC was modified with PEG derivatives (Numata et al. 2017).

For BCL-based samples, higher values of stress and strain were obtained compared with the blank samples (Fig. 5b) thus revealing a great mechanical improvement of the BCL modified with polymers. The BCL-PEGDA700 and BCL-PEGMA1100 registered close values of strain while BCL-PEGDA700 registered the highest values in terms of stress probably due to the chemical structure of PEGDA700 and the two active polymerizable sites. Moreover, these samples registered two times higher stress values than the blank sample. It is worth mentioning that the results obtained on Titan 2 Instrument are in accordance with the ones obtained on Discovery 850 DMA Instrument, also offering complementary information on the stress values at break.

DMA analysis of the BCF-polymer materials in the − 30 to + 115 °C temperature range

Considering that our study was aimed to offer an alternative for plastic packaging, DMA mechanical tests were performed on a larger temperature range (−30 to + 115 °C, with 5 °C /min heating rate). Thus, the films with

Table 2 Tensile tests performed for BC films and lyophilized BC modified with PEG derivatives

Sample code	Stress values (σ) in MPa compared at **STRAIN value of ε = 0.25%***	Young Modulus** MPa (E = σ/ε)
BCF	7.7	30.8
BCF-PEGDA700	9.7	38.8
BCF-PEGMA475	9.9	39.6
BCF-PEGMA1100	8.8	35.2
BCL	1.38	0.53
BCL-PEGDA700	1.26	0.48
BCL-PEGMA475	1.17	0.46
BCL-PEGMA1100	0.88	0.33

*ISO 527-2 defines modulus as the slope of the curve between 0.05 and 0.25% strain, calculated using either a chord or a linear regression slope calculation. However, since pre-stresses are applied to the material to remove any slack or compressive forces induced from gripping the specimen, comparing the samples at 0.25% strain should be more correct

** Average values were reported

approx. 36 mm × 12 mm × 0.5 mm ± 0.5 mm dimensions were analyzed to determine the viscoelastic properties for all BCF based samples. Therefore, Fig. 6 displays comparative plots on the variation of storage modulus, loss modulus and tan delta, respectively, as a function of temperature.

As expected, all BC films modified with polymeric matrices displayed significantly decreased values for storage modulus in comparison with neat BC films, being one order of magnitude lower (Fig. 6a). These lower values resulted due to their amorphous nature, suggesting the fact that these polymeric matrices led to a higher flexibility of the BC films while neat BC exhibited a higher rigidity due to the higher crystallinity of BC (Figueiredo et al. 2013). Similar trends were observed for temperature-dependent curves describing the loss modulus in Fig. 6a.

The BCF-PEGDA700, BCF-PEGMA475 and BCF-PEGMA1100 samples registered larger tan delta values (Fig. 6b), which demonstrate their capacity to dissipate more of the absorbed energy as a result of their increased elasticity compared with the blank sample. Thus, the presence of polymer matrix allowed a more efficient energy dissipation mechanism because the polymeric chains make these materials more resistant to the deformations which packaging materials are usually subjected to. In Figure S4a (*Supplementary file*), the storage modulus, the loss modulus and tan(δ) for neat BC films were plotted as a function of the temperature, demonstrating once again the damping behavior of blank samples that are more rigid compared to the hybrid ones.

In the case of the BCL-based materials, the same analysis was performed to investigate the mechanical performance of the samples in the same temperature range and under similar conditions (− 30 to + 115 °C, with 5°C/min heating rate). Figure S4b from *Supplementary file* revealed the storage and loss moduli as a function of temperature for the BCL and BCL-polymer based samples. In this case, the storage and loss moduli of all BCL-polymer based samples registered higher values compared with blank. Although this analysis proves that the polymer-based materials are more flexible compared with BCL, the curves possessed a diverging behavior (a non-linear tendency) which could be attributed to the higher porosity of these samples.

TGA analysis of the BC-polymer materials

TGA analysis could give important information related to the thermal stability of the samples and could reveal interesting interactions between the BC fibers and the grafted polymer chains. The TGA analysis was performed on the BC-polymer based materials obtained from BCF as blank. Also, the grafting degree was evaluated for the BCF modified samples.

Thus, the TGA analysis was performed for the BCF-polymer materials in order to determine the thermal behavior of the pristine and polymer modified BC materials. In Fig. 7 the thermogravimetric

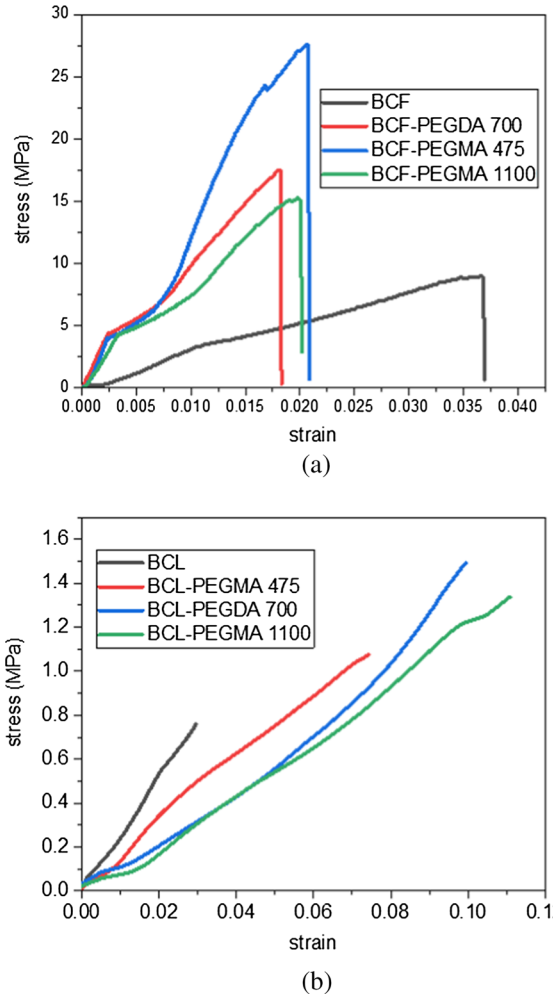

Fig. 5 Stress–strain plots for samples resulted from the modification of BCF (**a**) and BCL (**b**) obtained by utilizing the tensile test setup on Titan 2 Instrument

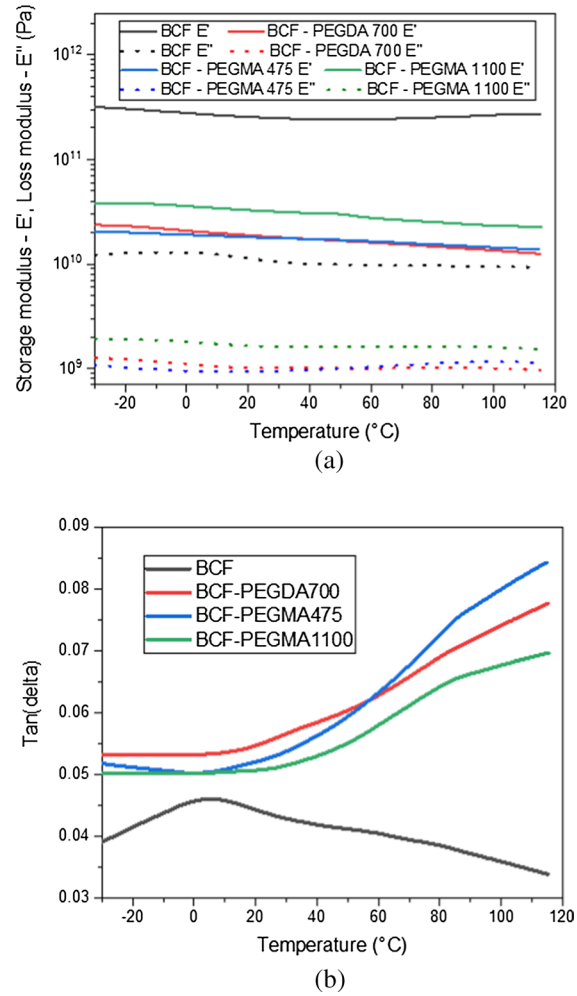

Fig. 6 Storage modulus (E') and Loss modulus (E") as a function of temperature (**a**) Tan delta (δ) as a function of temperature (**b**)

analyses, were recorded from room temperature to 900 °C. For pristine BCF the first temperature interval from room temperature to 130 °C is characterized by minor weight loss of 3.65% that can be explained by the endothermic signal corresponding to the moisture adsorbed on the surface of the sample (Fig. 7b).

The second significant weight loss occurs between 200 and 400 °C for BCF blank sample and was attributed to the exothermic degradation of cellulose and decomposition of glucose units which led to a 51.42% weight loss (Mohammadkazemi et al. 2015). The third weight loss of 18.07% for BC film was registered between 450 and 900 °C and it was associated with a more crystalline form of BC and the remaining pyrolysis content after temperature rises above 550 °C (Mohite and Patil 2014; Vazquez et al. 2013) (Fig. 7a, b). Thus, the total residual mass of BCF was 26.86%.

To determine the grafting degree for each polymer-based sample we considered the first and second weight loss steps registered at 130 °C and 256 °C.

The BCF-based materials registered a transition step (endothermic peak) (Fig. 9b) between room temperature and 130 °C which is attributed to the moisture adsorbed on the surface. Thus, the moisture adsorbed by each polymer-BCF based sample was 1.29% for BCF-PEGDA700, 2.87%

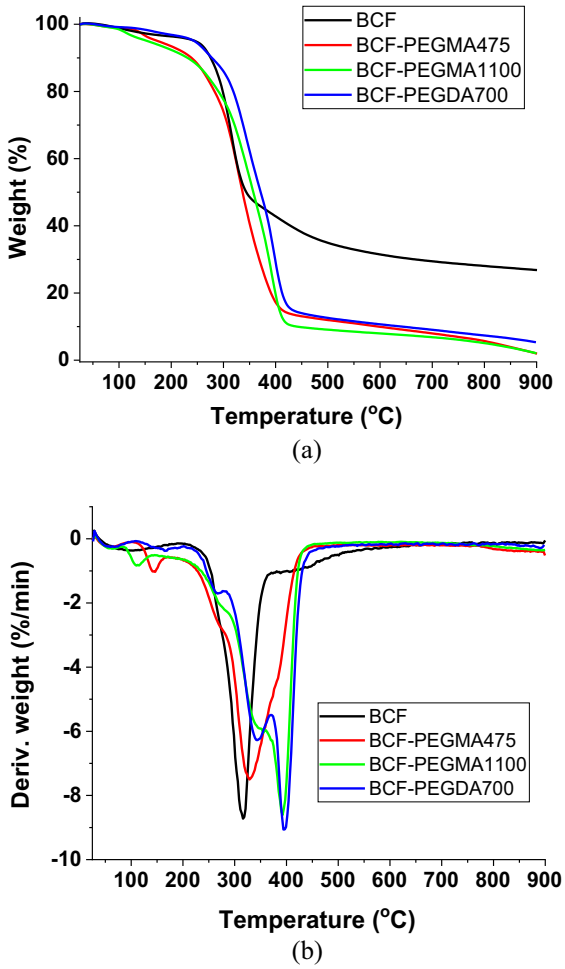

Fig. 7 Thermogravimetric analysis of pristine and BC-polymer based materials **a** TGA curve, and **b** DTG curve

for BCF-PEGMA475, respectively 2.15% for BCF-PEGMA1100.

To assess the grafting degree, a second weight loss step was observed around 256 °C for all types of polymer-based specimens. The total weight loss registered for the blank sample at 256 °C was 5.79%, while for the other specimens it was 6.3% for BCF-PEGDA700, 12.87% for BC-PEGMA475, respectively 12.89% for BC-PEGMA1100. Subtracting the values registered for adsorbed moisture for each sample and the weight loss of the blank sample (along with the corresponding adsorbed moisture of 3.65% determined previously) the grafting degree was minimum 2.87% for BCF-PEGDA700, 7.86% for BCF-PEGMA475, respectively 8.6% for BCF-PEGMA1100.

For the BCF-polymer based materials, the next weight loss was observed between 256 and 400 °C temperature range which corresponds to an altered thermal stability of the hybrid materials corresponding to the degradation of the cellulose and the start of polymer decomposition (Neblea et al. 2022). There was no significant difference between the hybrid samples, the registered weight loss values being 83.68% for BCF-PEGDA700, 81.68% for BCF-PEGMA475 and 86.27% for BCF-PEGMA1100. Also, the temperature range of the endothermic peaks was shifted from 260 to 320 °C in the case of blank sample to 325–400 °C for the BCF-polymer based materials confirming a very good heat stability (maximum at 390 °C) (Fig. 7b). For BCF-PEGMA475 the thermal stability was lower compared with the other BC samples modified with PEG derivatives (maximum peak value of 325 °C), this being attributed to the low molecular weight of the polymer chains. Thus, the thermal stability increased as the molecular weight of the PEG/oligo(ethylene)glycol derivatives was increased. This could be also correlated with SEM analysis since BCF-PEGMA475 had a different morphology in which polymer particles were covering the surface of BC, while in the other two cases compact, uniform structures of the samples were obtained.

The last transition step that appears in the case of hybrid samples from 450 to 900 °C is related to the degradation of the crystalline form of BC being similar to the TGA curves of the BCF blank sample, but the total residual mass of the BCF-polymer materials was lower probably due to a lower crystallinity of the samples attributed to the strong attachment of polymer chains to the BC fibers (Cai and Kim 2010). Thus, the residual mass was 5.34% for BCF-PEGDA700, 2.03% for BCF-PEGMA475, and 2.1% for BCF-PEGMA1100.

Degradation results obtained for BC-polymer materials

As presented in the Materials and Methods section, after 7, respectively 34 days of direct contact of the samples with the mold strains the BC-based samples were extracted from the nutrient medium and maintained in the same incubation conditions. In this way, the molds will be forced to use glucose as the only carbon source from BC. The degradation process was monitored by weighting the blank and BC-based

polymer materials at 7, 14, 34, 45 and 80 days after exposure to molds. The mass loss was plotted against time to evidence the degradation rate of the samples expressed as the slope of the curves.

(a) **Degradation results after 7 days**

In Figs. 8 and 9, the first two weight measurements represent the initial weight of the sample, respectively the weight of the sample covered by mold after extraction from the nutrient medium. The degradation rate was calculated as the slope of the curves which could be an indicator for the affinity of the mold to the substrate represented by the BC modified with polymer. To determine the degradation rate, the initial weight of the samples was not taken into consideration due to the samples loading with molds mycelium after 7 days that led to the increase of samples weight. After this exposure, some samples registered a weight decrease with time that was influenced differently depending on the mold strain.

In Fig. 8, after 7 days of exposure to the molds, the samples BCF-PEGDA700 and BCF-PEGMA475 had similar characteristics in terms of the degradation process compared with the BCF blank sample, regardless of the mold strain. Additionally, the

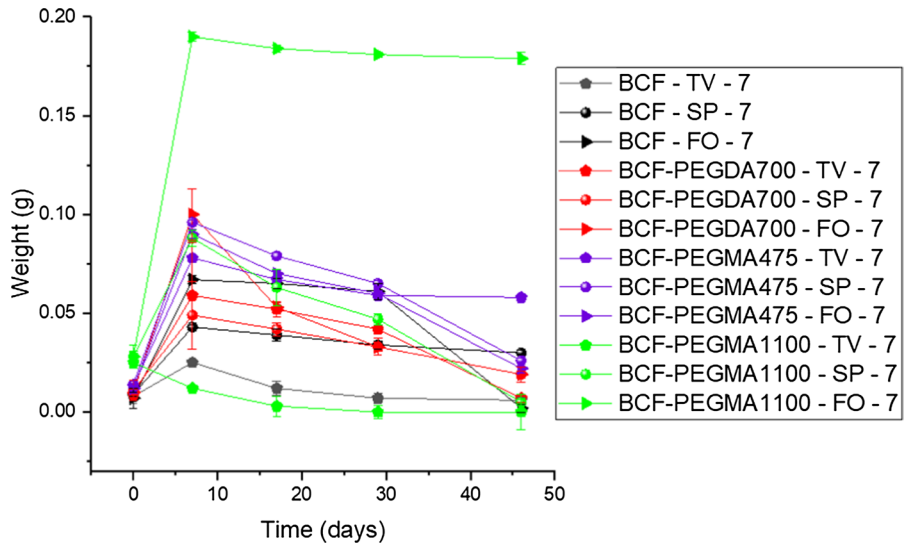

Fig. 8 The degradation process monitored by weight loss for BCF- polymer based materials and their blank counterparts after exposure to *Trichoderma viridae* (TV), *Sporotrichum pulverulentum* (SP) and *Fusarium oxysporum* (FO) for 7 days (details of standard deviation—Table S5—Supplementary File)

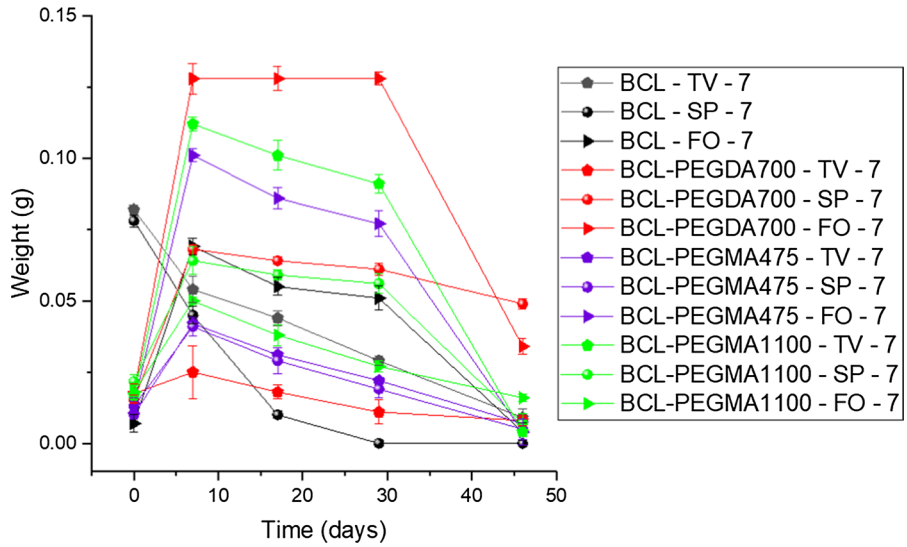

Fig. 9 The degradation process monitored by weight loss for BCL- polymer based materials and their blank counterparts after exposure to *Trichoderma viridae* (TV), *Sporotrichum pulverulentum* (SP) and *Fusarium oxysporum* (FO) for 7 days (details of standard deviation—Table S6—Supplementary File)

degradation rate was higher for these samples in comparison with the blank BC films. To do this comparison more accurately in Table S1—*Degradation rate values for BCF-based samples* from *Supplementary information* the values of the degradation rate were determined. The degradation rates, namely the slopes of the curves, were calculated through the tendency lines; for the interpretation of the results, the values of the slopes in module were considered. In some cases, not all experimental points fitted a linear tendency, but a polynomial tendency. In these cases, in which a quadratic or cubic polynomial tendency line best fitted the experimental points, the slope (the degradation rate) was obtained after applying the linear tendency to these curves (details in the last column of Table S1).

The value in module of the slope could be attributed to the mold affinity for these samples that were used as carbon source for the survival behavior of the strain. In the case of BCF modified with PEGMA1100 the behavior of the material was highly different in the presence of *F. oxysporum (*Fig. 8—*sample BC-PEGMA1100-FO-7)* compared with the BCF modified with PEGDA700 or PEGMA475. Due to the nature of the polymer functionality and the compact film structure according to SEM micrographs (Figure S7-Supplementary information) and the morphology of the colony of *F. oxysporum* the loading degree was probably very high, while the degradation rate was considerably lower compared with the other two types of BCF-polymer based materials exposed to the same strain (Table S1).

However, the aspect of sample BCF-PEGMA1100-FO-7 was completely different among all samples considering the high humidity of this sample that prevented the performing of SEM analysis (Figure S7—the corresponding SEM image for this sample is missing). Therefore, in the case of these samples, we have decided to analyse the degradation process after 34 days.

After 7 days of exposure to *S. pulverulentum*, the highest degradation rate was registered for BCF-PEGMA1100 (slope in module was $2.06{\cdot}10^{-3}$ g/days—Table S1-*Supplementary information*), while the lower degradation rate was registered by blank sample BCF-SP-7. Probably the microorganisms' hyphae of *S. pulverulentum* protruded in the compact structure and led to a higher degradation rate of the BCF-PEGMA1100 compared with the blank BCF exposed to the same strain. For *T. viridae* the samples had very close values of the slopes except BCF-PEGDA-700 which registered a value of the slope one order of magnitude higher compared with the rest of the samples.

To conclude, the results of the degradation process after 7 days, it can be observed that from Table S1 (*Slope column—Supplementary information*) that among all samples exposed to the three types of molds, sample BC-PEGMA1100-SP-7 had the highest value of the degradation rate. Although BC is by itself a biodegradable material, the grafted PEGMA1100 chains determined an acceleration of the degradation process compared with the blank material which is a great result in terms of designing biodegradable materials with higher degradation rates that could contribute to a cleaner environment.

Based on the allure of the curves from Fig. 9, for the lyophilized BC-polymer based materials the strains heavily adapted to the porous structure of the samples in all cases probably due to a higher polymer coverage degree induced by the polymer chains grafted onto the more loosen structure of BC fibrils based on the allure of the curves from Fig. 9. Thus, it was noticed that the highest degradation rate was registered for the BCL blank sample in the presence of *S. pulverulentum* (slope value in module $4.26\times{\cdot}10^{-3}$ g/days) in Table 3.

In some cases, regardless of the mould or the BC-polymer based materials, there was a delay in the degradation process since most of the samples had similar weight values for almost 30 days which can be attributed to the growth lag period of the moulds (allure of the curves from Fig. 9).

Although the porous structure of the samples could favor the extension of the hyphae inside of the lyophilized BC-polymer based materials the results revealed that the strains were unable to reach the carbon source due to fully coverage of the fibrils with polymer confirmed by SEM analysis (Fig. 1—top and cross-section images—*Manuscript*) in all cases. Therefore, only the blank BCL samples had registered the highest degradation rates compared with the BCL-polymer based materials and also with the BCF blank samples regardless of the strain type, results confirmed by comparing the slope values from Table 3.

Also, higher degradation rates were registered for samples BCL-PEGMA475 and BCL-PEGMA1100

Table 3 Degradation rates of the BCF and BCL-polymer based materials after 7 days of exposure to the three types of molds

Sample code	Slope/Degradation rate	Sample	Slope/Degradation rate
BCF-TV-7	-4.4×10^{-4}	BCL-TV-7	-1.45×10^{-3}
BCF-SP-7	-3.38×10^{-4}	BCL-SP-7	-4.26×10^{-3}
BCF-FO-7	-2.75×10^{-4}	BCL-FO-7	-1.57×10^{-3}
BCF-PEGDA-700-TV-7	-1.31×10^{-3}	BCL-PEGDA700-TV-7	-4.34×10^{-4}
BCF-PEGDA-700-SP-7	$-7.71-4$	BCL-PEGDA700-SP-7	-4.76×10^{-4}
BCF-PEGDA-700-FO-7	-1.65×10^{-3}	BCL-PEGDA700-FO-7	-2.11×10^{-18}
BCF-PEGMA-475-TV-7	$-5.14\times\cdot10^{-4}$	BCL-PEGMA 475-TV-7	-8.80×10^{-4}
BCF-PEGMA-475-SP-7	-1.76×10^{-3}	BCL-PEGMA 475-SP-7	-9.06×10^{-4}
BCF-PEGMA-475-FO-7	$-1.68\cdot\times10^{-3}$	BCL-PEGMA 475-FO-7	-1.08×10^{-3}
BCF-PEGMA-1100-TV-7	-4.98×10^{-4}	BCL-PEGMA 1100-TV-7	-9.51×10^{-4}
BCF-PEGMA-1100-SP-7	-2.06×10^{-3}	BCL-PEGMA 1100-SP-7	-3.60×10^{-4}
BCF-PEGMA-1100-FO-7	$-2.67\cdot\times10^{-4}$	BCL-PEGMA 1100-FO-7	-8.61×10^{-4}

exposed to *T. viridae* compared with the same grafted polymers but using BCF as support. Similar behavior was registered in the case of BCL-PEGMA1100 exposed to *F. oxysporum* that had a higher slope value in module compared with BCF-PEGMA1100 exposed to the same strain (Table 3 and detailed results in Tables S1 and Table S2). Nevertheless, regardless of the grafted polymer chains onto the BCL the presence of the polymer did not led to an acceleration of the degradation rate as in the previous case, thus the lyophilized blank samples being degraded faster irrespective of the selected strain.

(b) **Degradation results after 34 days**

As presented above, some samples registered an accelerated degradation rate after the grafting process, while others had lower values of the degradation rates after 7 days of exposure to different types of molds. Thus, our next step was to investigate the behavior of the samples after 34 days of exposure to the three types of strains.

In the case of the samples exposed for 34 days to the same molds (Figure S5), we first noticed that the degradation rate increased for the BCF blank samples in all cases compared with those exposed for 7 days (compared values of the slopes assessed in Table 4—*details in Tables S1 and S3*).

Another interesting aspect was observed in the case of the samples degraded in the presence of *T.*

Table 4 Slope comparison of BCF-based samples after 7, respectively 34 days of exposure to the three types of molds

Sample code	Slope/Degradation rate	Sample	Slope/Degradation rate
BCF-TV-7	-4.4×10^{-4}	BCF-TV-34	$-8.16\times\cdot10^{-4}$
BCF-SP-7	-3.38×10^{-4}	BCF-SP-34	-4.15×10^{-4}
BCF-FO-7	-2.75×10^{-4}	BCF-FO-34	-5.19×10^{-4}
BCF-PEGDA-700-TV-7	-1.31×10^{-3}	BCF-PEGDA-700-TV-34	-1.73×10^{-4}
BCF-PEGDA-700-SP-7	$-7.71-4$	BCF-PEGDA-700-SP-34	-1.13×10^{-4}
BCF-PEGDA-700-FO-7	-1.65×10^{-3}	BCF-PEGDA-700-FO-34	-5.5×10^{-3}
BCF-PEGMA-475-TV-7	-5.14×10^{-4}	BCF-PEGMA-475-TV-34	-5.63×10^{-4}
BCF-PEGMA-475-SP-7	-1.76×10^{-3}	BCF-PEGMA-475-SP-34	-8.52×10^{-4}
BCF-PEGMA-475-FO-7	-1.68×10^{-3}	BCF-PEGMA-475-FO-34	-1.31×10^{-3}
BCF-PEGMA-1100-TV-7	-4.98×10^{-4}	BCF-PEGMA-1000-TV-34	-9.23×10^{-4}
BCF-PEGMA-1100-SP-7	-2.06×10^{-3}	BCF-PEGMA-1000-SP-34	-1.76×10^{-4}
BCF-PEGMA-1100-FO-7	-2.67×10^{-4}	BCF-PEGMA-1000-FO-34	-1.07×10^{-3}

viridae, considering that after 34 days of exposure, sample BCF-PEGDA700 registered the highest degradation rate compared with all the other samples. This could be explained by the necessity of this strain to produce the cellulase enzyme which requires more time. Thus, to enhance the degradation of these materials in the presence of *T. viridae* a longer exposure time is necessary. The samples exposed to *S. pulverulentum* registered lower degradation rates, BCF-PEGDA700 having the lowest slope value compared with all the other samples (Table 4) which can be attributed to the low excretion of cellulase although the loading of micelles was high on the surface of the sample.

On the other hand, in the case of grafted PEGMA475, respectively PEGMA1100, the BCF-polymer based materials registered the highest degradation rates in the presence of *S. pulverulentum* which can be explained by two facts: **i)** the polymer is not fully covering the BCF, thus the cellulase enzymes have access to the BC matrix and **ii)** the more hydrophilic characteristic of the PEGMA grafted chains accelerate the degradation process.

For *F. oxysporum*, the highest degradation rates were registered for the BCF samples modified with PEGMA475 and PEGMA1100. These samples had the lowest values of the contact angle, being more hydrophilic compared with the blank sample and BCF-PEGDA700 which could be an indication of higher activity of the mould since the material could retain more water from the cultivation media due to its more hydrophilic characteristic being corelated also with the contact angle measurements. Nevertheless, the degradation results are not completely correlated with previous ones obtained after exposure of 7 days due to probably the diminished exposure period to *F. oxysporum*.

For samples obtained from lyophilized BC, after 34 days (Figure S6), the hierarchy of the degradation rates of the blank samples has changed compared with those exposed to 7 days, the higher value of the degradation rate being registered after exposure to *T. viridae* for sample BCL-PEGMA1100-TV-34 (Table 5).

Higher values of the degradation rates were registered for the BCL modified with PEGDA700 after 34 days of exposure to *T. viride* and *S. pulverulentum* compared with the samples exposed to 7 days (Table 5) which can be attributed to a longer period for cellulase excretion for these two strains (Enari and Markkanen 1977).

However, the grafts of PEGMA475 and PEGMA1100 had a different effect on the degradation process. In the case of BCL-PEGMA475 lower values of the degradation rate were obtained after 34 days in the case of *T. viridae* and *S. pulverulentum*, while in the case of *F. oxysporum* there were no drastic changes compared with the samples exposed for 7 days to the same strains (Table 5). Similar behavior was noticed for the same BCL-PEGMA1100 exposed to *F. oysporum* for 34 days since there were not significant differences between the degradation rate registered after 34 days compared to the one registered after 7 days. For the same sample, *S. pulverlentum*

Table 5 Degradation rates for BCL-based samples after 7, respectively 34 days of exposure to the three types of moulds

Sample code	Slope/Degradation rate	Sample	Slope/Degradation rate
BCL-TV-7	-1.45×10^{-3}	BCL-TV-34	-2.12×10^{-3}
BCL-SP-7	-4.26×10^{-3}	BCL-SP-34	-1.79×10^{-4}
BCL-FO-7	-1.57×10^{-3}	BCL-FO-34	-3.64×10^{-4}
BCL-PEGDA700-TV-7	-4.34×10^{-4}	BCL-PEGDA700-TV-34	-6.71×10^{-4}
BCL-PEGDA700-SP-7	-4.76×10^{-4}	BCL-PEGDA700-SP-34	-7.27×10^{-4}
BCL-PEGDA700-FO-7	-2.11×10^{-18}	BCL-PEGDA700-FO-34	-2.08×10^{-4}
BCL-PEGMA 475-TV-7	-8.80×10^{-4}	BCL-PEGMA 475-TV-34	-1.19×10^{-4}
BCL-PEGMA 475-SP-7	-9.06×10^{-4}	BCL-PEGMA 475-SP-34	-2.22×10^{-4}
BCL-PEGMA 475-FO-7	$-1.08\times\cdot10^{-3}$	BCL-PEGMA 475-FO-34	$-1.05\times\cdot10^{-3}$
BCL-PEGMA 1100-TV-7	-9.51×10^{-4}	BCL-PEGMA 1100-TV-34	-1.74×10^{-3}
BCL-PEGMA 1100-SP-7	-3.60×10^{-4}	BCL-PEGMA 1100-SP-34	-1.98×10^{-4}
BCL-PEGMA 1100-FO-7	-8.61×10^{-4}	BCL-PEGMA 1100-FO-34	-7.00×10^{-4}

registered lower values of the slope after 34 days, while *T. viridae* had an opposite behaviour attributed to the same retardation of cellulase excretion since lower values of the degradation rate were obtained.

Nevertheless, the polymer grafts did not accelerate the degradation rates in the case of lyophilized samples compared with those obtained by BC film pellicles. Probably this is due to the imperfection of the polymer film (not completely evidenced by SEM analysis in Fig. 2 that covers the surface of BC films leading to the intrusion of mold hyphae in the structure of the material and also to the hydrophilic nature of the polymers that favored the diffusion of cellulase excreted by the strains.

SEM analysis of the BC-polymer based materials after degradation

To investigate the aspect of the BC-polymer based materials covered by the three types of molds the samples were analyzed by SEM. Regardless of the initial state of BC (lyophilized or film) and of the grafted polymer chains the samples were covered completely by the molds (Figure S7 and Figure S8 from *Supplementary information*).

In the case of BCL-polymer based materials, compared with the blank samples, the initial structure of these materials was no longer observed except for sample BCL-PEGDA700-SP in which some parts of the material surface are still visible (Figure S7). Here, the aerial hyphae are distributed on the surface of the material, while the vegetative hyphae probably infiltrated inside the material through the pores that were evidenced in Fig. 1d for the initial form of the BCL-PEGDA700 material.

For BCL-blank, *T. viridae* extended its hyphae more on the surface of the material, while in the case of BCF-blank its hyphae seem to be integrated in the film structure. Comparing the growth aspect of *S. pulverulentum* a porous lamellar structure of pristine BCL determines a layered structure of the mycelium (Figure S8) which is not observable in the case of BCF blank material. The BC film has a compact lamellar structure evidenced by the cross-section micrograph image (Fig. 2a) that determines a 3D growth of the same mold mycelium (Figure S7). An interesting behavior was noticed in the case of *F. oxysporum* that generated sporulated aerian hyphae in the case of BC films (Figure S7- BCF-blank-FO), while in the case of BCL the whole mycelium is situated on the surface of the blank material (Figure S8—BCL-blank-FO).

For BC-PEGDA700 the aspect of the samples is not significantly different compared with the blank samples in the presence of the three types of mold. A similar growth aspect was evidenced by the SEM images in all cases with some differences related to the amount of mould's mycelium distributed on the materials surface (*i.e.:* BCL-PEGDA700-SP vs. BCL-blank-SP).

In the case of BCF and BCL modified PEGMA derivatives the aspect of the materials was different after the exposure to the three types of molds which could be attributed to the grafting degree of the polymer chains, their molecular weight and also to the hydrophilic characteristic of the final materials. Thus, for BCL-PEGMA475 the sporulation process was delayed comparing with BCL-PEGMA1100 (correlated with the degradation rate—Fig. 9) for all types of strains.

Samples BCF-PEGMA475 and BCF-PEGMA1100 exposed to *T. viridae* the material presents embedded spores on the surface (Figure S7). *S. pulverulentum* presents a higher sporulation process in the case of BCF-PEGMA1100, while for BCF-PEGMA475, probably due to lower molecular weight of OEGMA475 the vegetative mycelium penetrates the material (Figure S7).

For sample BCF-PEGMA1100-FO-7 the SEM micrograph was not depicted due to the consistency of the sample after the exposure to *F. oxysporum* after 7 days (SEM image missing in Figure S8). The sample was characterized by high humidity and the SEM analysis was impossible to be performed. This behavior is related with the more hydrophilic characteristic of the samples modified with OEGMA1100 that started to accelerate the process of degradation that was more evident after 34 days of exposure to *F. oxysporum*. Thus, the SEM analysis are in good agreement with the degradation rates mathematically determined, since the value in module of the degradation rate after exposure to 34 days (Table S3—sample BCF-PEGMA1100-FO-34) was much higher compared with the one obtained after 7 days of exposure (Table S1– sample BCF-PEGMA1100-FO-34).

On the other hand, *F. oxysporum* presents a different morphology of the spores comparatively with all other cases since the degradability rate was higher for

BCL-PEGMA1100-FO-7 (higher value of the slope in Table S2 compared with Table S4) and the desiccation process was strong since we were not able to perform SEM analysis for BCF-PEGMA1100 (Figure S8).

Conclusions

In conclusion, new functional materials for future biodegradable food packaging were obtained by grafting three types of PEG derivatives with different molecular weights (PEGDA700, PEGMA475 and PEGMA1100) onto the BC matrix through radical polymerization.

The blank samples and BC-polymer based materials were analyzed by SEM, FT-IR, contact angle measurements, and TGA. Tensile tests and DMA analysis were used to compare the polymer-BCL, respectively polymer-BCF types of materials in terms of shear-modulus, tensile strength and degradation performance giving suitable information for food packaging applications.

As expected, the BCF-PEGMA475 and BCF-PEGMA1100 materials had a more hydrophilic characteristic compared with the blank sample and BCF-PEGDA700, while the contact angle measurements for the polymer-based BCL specimens were inconclusive due to the higher porosity of the samples.

All samples registered higher values of G' storage modulus and lower values for G'' loss modulus in the whole frequency range. In terms of tensile mechanical tests BCF-PEGMA 1100 proved optimal mechanical performances, possessing both high resistance and also a slightly higher stretchability compared with all other samples. The DMA analysis (performed on a temperature range from − 30 °C to + 110 °C) demonstrated that all BCF modified with PEG derivatives displayed significantly lower values for storage modulus in comparison with blank sample.

A new degradation method was proposed to give quantitative information about the degradation process after 7, respectively 34 days of exposure to three types of molds.

The evaluation of the degradation rates of the samples demonstrates that in the case of BCF-based materials, the modification with PEG derivatives of higher molecular weight led to an accelerated degradation process compared to pristine samples.

Also, the SEM micrographs performed for the degraded samples were in good agreement with the proposed mathematical method for the evaluation of the degradation process.

In conclusion, the mechanical and biodegradability results for the BCF-PEGMA1100 bring new and valuable information for future decomposable food packaging.

Acknowledgments This work was financially granted by the Ministry of Research, Innovation and Digitalisation (UEFISCDI) through PN-III-P2-2.1-PED-2021− ctr.no. 672PED/2022. Aurel Diacon gratefully acknowledges financial support from the Competitiveness Operational Program 2014-2020, Action 1.1.3: Creating synergies with RDI actions of the EU's HORIZON 2020 framework program and other international RDI programs, MySMIS Code 108792, Acronym project "UPB4H", financed by contract: 250/11.05.2020. The APC was funded by University Politehnica of Bucharest, within the PubArt Program.

Author contributions Idea, conceptualization and validation were performed by ER and AM Material preparation and data collection were performed by AM and AD (Aurel Diacon). Analysis of the materials was performed by GI, GT, AD (Aurel Diacon), and AD (Adrian Dinescu). The manuscript and the figures were prepared by AM, GT and GI All authors reviewed the manuscript.

Funding The authors have not disclosed any funding.

Data availability Details related to mechanical tests and the degradation process after 34 days are included in Supplementary file.

Declarations

Conflict of interest The authors have no financial or non-financial interests to disclose.

Ethics approval Not applicable.

Consent to participate Not applicable.

Consent for publication The authors have given their consent for publication and disclose their personal data.

References

Bhardwaj U, Dhar P, Kumar A, Katiyar V (2014) Polyhydroxyalkanoates (PHA)-cellulose based nanobiocomposites for food packaging applications. In: Komolprasert V, Turowski P (eds) Food additives and packaging, ACS Symposium Series, 1st edn. American Chemical Society, Washington, DC, pp 275–314

Blanco Parte FG, Santoso SP, Chou C-C, Verma V, Wang H-T, Ismadji S, Cheng K-C (2020) Current progress on the production, modification, and applications of bacterial cellulose. Crit Rev Biotechnol 40:397–414. https://doi.org/10.1080/07388551.2020.1713721

Byun Y, Kim YT (2014) Bioplastics for food packaging: chemistry and physics. In: Han JH (ed) Innovations in food packaging, 2nd edn. Academic Press, pp 353–368

Cai Z, Kim J (2010) Bacterial cellulose/poly(ethylene glycol) composite: characterization and first evaluation of biocompatibility. Cellulose 17:83–91. https://doi.org/10.1007/s10570-009-9362-5

Chen WH, Wang CW, Ong HC, Show PL, Hsieh TH (2019) Torrefaction, pyrolysis and two-stage thermodegradation of hemicellulose, cellulose and lignin. Fuel 258:116168. https://doi.org/10.1016/j.fuel.2019.116168

Chen C, Ding W, Zhang H, Zhang L, Huang Y, Fan M, Yang J, Sun D (2022) Bacterial cellulose-based biomaterials: from fabrication to application. Carbohydr Polym 278:118995. https://doi.org/10.1016/j.carbpol.2021.118995

Choi SM, Shin EJ (2020) The nanofication and functionalization of bacterial cellulose and its applications. Nanomaterials 10:406. https://doi.org/10.3390/nano10030406

Dîrloman FM, Toader G, Rotariu T, Ţigănescu TV, Ginghină RE, Petre R, Alexe F, Ungureanu MI, Rusen E, Diacon A, Ghebaur A, Duldner M, Coman AE, Ţincu R (2021) Novel polyurethanes based on recycled polyethylene terephthalate: synthesis, characterization, and Formulation of binders for environmentally responsible rocket propellants. Polymers 13:3828. https://doi.org/10.3390/polym13213828

Dobre T, Stoica A, Pârvulescu OC, Stroescu M, Iavorschi G (2008) Factors influence on bacterial cellulose growth in static reactors. Rev Chim-Bucharest 59:191–195. https://doi.org/10.37358/RC.08.5.1835

Dong Z, Hou X, Sun F, Zhang L, Yang Y (2014) Textile grade long natural cellulose fibers from bark of cotton stalks using steam explosion as a pretreatment. Cellulose 21:3851–3860. https://doi.org/10.1007/s10570-014-0401-5

Enari TM, Markkanen P (1977) Production of cellulolytic enzymes by fungi. Advances in biochemical engineering, vol 5. Springer, Berlin, Heidelberg, pp 1–24

Figueiredo AGPR, Figueiredo ARP, Alonso-Varona A, Fernandes SCM, Palomares T, Rubio-Azpeitia E, Barros-Timmons A, Silvestre AJD, Pascoal Neto C, Freire CSR (2013) Biocompatible bacterial cellulose-poly(2-hydroxyethyl methacrylate) nanocomposite films. BioMed Res Int 2013:698141. https://doi.org/10.1155/2013/698141

Ghaderi M, Mousavi M, Yousefi H, Labbafi M (2014) All-cellulose nanocomposite film made from bagasse cellulose nanofibers for food packaging application. Carbohydr Polym 104:59–65. https://doi.org/10.1016/j.carbpol.2014.01.013

Hong LG, Yuhana NY, Zawawi EZE (2021) Review of bioplastics as food packaging materials. AIMS Mater Sci 8:166–184. https://doi.org/10.3934/matersci.2021012

Jang WD, Kim TY, Kim HU, Shim WY, Ryu JY, Park JH, Lee SY (2019) Genomic and metabolic analysis of Komagataeibacter xylinus DSM 2325 producing bacterial cellulose nanofiber. Biotechnol Bioeng 116:3372–3381. https://doi.org/10.1002/bit.27150

Khan B, Bilal Khan Niazi M, Samin G, Jahan Z (2017) Thermoplastic starch: a possible biodegradable food packaging material—a review. J Food Process Eng 40:e12447. https://doi.org/10.1111/jfpe.12447

Kongkaoroptham P, Piroonpan T, Pasanphan W (2021) Chitosan nanoparticles based on their derivatives as antioxidant and antibacterial additives for active bioplastic packaging. Carbohydr Polym 257:117610. https://doi.org/10.1016/j.carbpol.2020.117610

Li Y, Tian Y, Zheng W, Feng Y, Huang R, Shao J, Tang R, Wang P, Jia Y, Zhang J, Zheng W, Yang G, Jiang X (2017) Composites of bacterial cellulose and small molecule-decorated gold nanoparticles for treating gram-negative bacteria-infected wounds. Small 13:1700130. https://doi.org/10.1002/smll.201700130

Marič L, Cleenwerck I, Accetto T, Vandamme P, Trček J (2020) Description of Komagataeibacter melaceti sp. Nov. and Komagataeibacter melomenusus sp. Nov. Isolated from Apple Cider Vinegar. Microorganisms 8:1178. https://doi.org/10.3390/microorganisms8081178

Mocanu A, Isopencu G, Busuioc C, Popa OM, Dietrich P, Socaciu-Siebert L (2019) Bacterial cellulose films with ZnO nanoparticles and propolis extracts: synergistic antimicrobial effect. Sci Rep 9:17687. https://doi.org/10.1038/s41598-019-54118-w

Mohammadkazemi F, Azin M, Ashori A (2015) Production of bacterial cellulose using different carbon sources and culture media. Carbohydr Polym 117:518–523. https://doi.org/10.1016/j.carbpol.2014.10.008

Mohite BV, Patil SV (2014) Physical, structural, mechanical and thermal characterization of bacterial cellulose by G. hansenii NCIM 2529. Carbohydr Polym 106:132–141. https://doi.org/10.1016/j.carbpol.2014.02.012

Mokhena TC, John MJ (2020) Cellulose nanomaterials: new generation materials for solving global issues. Cellulose 27:1149–1194. https://doi.org/10.1007/s10570-019-02889-w

Moon RJ, Martini A, Nairn J, Simonsen J, Youngblood J (2011) Cellulose nanomaterials review: structure, properties and nanocomposites. Chem Soc Rev 40:3941–3994. https://doi.org/10.1039/C0CS00108B

Moore EM, West JL (2019) Bioactive poly(ethylene glycol) acrylate hydrogels for regenerative engineering. Regen Eng Transl Med 5:167–179. https://doi.org/10.1007/s40883-018-0074-y

Morris VB, Nimbalkar S, Younesi M, Mcclellan P, Akkus O (2017) Mechanical properties, cytocompatibility and manufacturability of Chitosan: pegda hybrid-gel scaffolds by stereolithography. Ann Biomed Eng 45:286–296. https://doi.org/10.1007/s10439-016-1643-1

Mülhaupt R (2013) Green polymer chemistry and bio-based plastics: dreams and reality. Macromol Chem Phys 214:159–174. https://doi.org/10.1002/macp.201200439

Neblea IE, Gavrila A-M, Iordache TV, Zaharia A, Stanescu PO, Radu I-C, Burlacu SG, Neagu G, Chiriac A-L, Sarbu A (2022) Interpenetrating networks of bacterial cellulose and poly (ethylene glycol) diacrylate as potential cephalexin carriers in wound therapy. J Polym Res 29:406. https://doi.org/10.1007/s10965-022-03250-9

Numata Y, Sakata T, Furukawa H, Tajima K (2015) Bacterial cellulose gels with high mechanical strength. Mater Sci Eng, C 47:57–62. https://doi.org/10.1016/j.msec.2014.11.026

Numata Y, Kono H, Tsuji M, Tajima K (2017) Structural and mechanical characterization of bacterial cellulose–polyethylene glycol diacrylate composite gels. Carbohydr Polym 173:67–76. https://doi.org/10.1016/j.carbpol.2017.05.077

Numata Y, Yoshihara S, Kono H (2021) In situ formation and post-formation treatment of bacterial cellulose/κ-carrageenan composite pellicles. Carbohy Polym Technol Appl 2:100059. https://doi.org/10.1016/j.carpta.2021.100059

Raghavendran V, Asare E, Roy I (2020) Bacterial cellulose: biosynthesis, production, and applications. Advances in microbial physiology, 1st edn. Academic Press, London, pp 89–138

Rebelo AR, Archer AJ, Chen X, Liu C, Yang G, Liu Y (2018) Dehydration of bacterial cellulose and the water content effects on its viscoelastic and electrochemical properties. Sci Technol Adv Mat 19:203–211. https://doi.org/10.1080/14686996.2018.1430981

Siracusa V, Rocculi P, Romani S, Rosa MD (2008) Biodegradable polymers for food packaging: a review. Trends Food Sci Technol 19:634–643. https://doi.org/10.1016/j.tifs.2008.07.003

Sun R, Tomkinson J (2005) Separation and characterization of cellulose from wheat straw. Sep Sci Technol 39:391–411. https://doi.org/10.1081/SS-120027565

Tsouko E, Kourmentza C, Ladakis D, Kopsahelis N, Mandala I, Papanikolaou S, Paloukis F, Alves V, Koutinas A (2015) Bacterial cellulose production from industrial waste and by-product streams. Int J Mol Sci 7:14832–14849. https://doi.org/10.3390/ijms160714832

Vadanan SV, Basu A, Lim S (2022) Bacterial cellulose production, functionalization, and development of hybrid materials using synthetic biology. Polym J 54:481–492. https://doi.org/10.1038/s41428-021-00606-8

Vazquez A, Foresti ML, Cerrutti P, Galvagno M (2013) Bacterial cellulose from simple and low cost production media by gluconacetobacter xylinus. J Polym Environ 21:545–554. https://doi.org/10.1007/s10924-012-0541-3

Wang P, Tan KL, Kang ET, Neoh KG (2001) Surface functionalization of low density polyethylene films with grafted poly(ethylene glycol) derivatives. J Mater Chem 11:2951–2957. https://doi.org/10.1039/B101974K

Zhang H, Xu X, Chen X, Yuan F, Sun B, Xu Y, Yang J, Sun D (2017a) Complete genome sequence of the cellulose-producing strain Komagataeibacter nataicola RZS01. Sci Rep 7:4431. https://doi.org/10.1038/s41598-017-04589-6

Zhang X, Zhang J, Dong L, Ren S, Wu Q, Lei T (2017b) Thermoresponsive poly(poly(ethylene glycol) methylacrylate)s grafted cellulose nanocrystals through SI-ATRP polymerization. Cellulose 24:4189–4203. https://doi.org/10.1007/s10570-017-1414-7

Zhao X, Cornish K, Vodovotz Y (2020) Narrowing the gap for bioplastic use in food packaging: an update. Environ Sci Technol 54:4712–4732. https://doi.org/10.1021/acs.est.9b03755

Zhijiang C, Chengwei H, Guang Y (2012) Poly(3-hydroxubutyrate-co-4-hydroxubutyrate)/bacterial cellulose composite porous scaffold: preparation, characterization and biocompatibility evaluation. Carbohydr Polym 87:1073–1080. https://doi.org/10.1016/j.carbpol.2011.08.037

Zhong C (2020) Industrial-scale production and applications of bacterial cellulose. Front Bioeng Biotechnol 8:605374. https://doi.org/10.3389/fbioe.2020.605374